Low-Complexity MIMO Multiuser Receiver: A Joint Antenna Detection Scheme for Time-Varying Channels

Charlotte Dumard, *Student Member, IEEE*, and Thomas Zemen, *Member, IEEE*

***Abstract*—This paper deals with the uplink of a wireless multiple-input multiple-output (MIMO) communication system based on multicarrier (MC) code division multiple access (CDMA). We focus on time-varying channels for users moving at vehicular speeds. The optimal maximum *a posteriori* (MAP) receiver for such a system is prohibitively complex and can be approximated using iterative linear minimum mean-square error (LMMSE) multiuser detection and parallel interference cancellation (PIC). For time-varying channels, two LMMSE filters for channel estimation and multiuser detection need to be computed at every time instant, making implementation in a real-time system difficult. We develop a novel low-complexity receiver that exploits the multiple antenna structure of the system and performs joint iterative multiuser detection and channel estimation. Our receiver algorithms are based on the Krylov subspace method, which solves a linear system with low complexity, trading accuracy for efficiency. The computational complexity of the channel estimator can be reduced by one order of magnitude. For multiuser detection, a PIC scheme in the *user space*, i.e., after the matched filter, allows simultaneous detection of all users as well as drastic computational complexity reduction by more than one order of magnitude.**

***Index Terms*—Joint antenna detection, Krylov subspace method, low-complexity receiver, multiple-input multiple-output (MIMO), orthogonal frequency-division multiplexing (OFDM), time-varying channel.**

I. Introduction

THIS paper deals with the uplink of a wireless multiple-input multiple-output (MIMO) communication system for users at vehicular speeds. The communication system is based on multicarrier (MC) code-division multiple access (CDMA). Receiver algorithms for such a system require high computational complexity due to the linear minimum mean-square error (LMMSE) filters employed for multiuser detection and channel estimation [1]–[3]. We develop a novel low-complexity receiver based on the Krylov subspace method.

The Krylov subspace method [4]–[7] allows to solve a linear system with low complexity by trading accuracy for efficiency. It has long been used in signal processing, e.g., for beamforming [8], [9] or detection [10], [11], where a computational complexity reduction is shown.

In [10], universal weights are computed, based on the self-averaging properties of random matrices modeling the channel. The *a priori* random eigenvalues of the channel matrix can be described by averaging over sufficiently large samples. The eigenvalue distribution of the channel matrix converges to a deterministic distribution when its dimensions grow to infinity. Universal weights are thus computed independently of the received signal. However, the authors in [10] do not take into account an iterative scheme using interference cancellation. In such a case, the projection computations are not common to all users anymore, and no computational complexity reduction can be achieved this way.

In [11], the authors use the Lanczos algorithm to approximate the Wiener filter in an iterative receiver for a *single-user* single-input multiple-output (SIMO) system. Their iterative scheme uses an adjusted mean of the signal based on *a priori* information to cancel the multipath interference. The computational complexity using the Lanczos algorithm in [11] scales quadratic with the length of the observation vector.

We aim at developing an efficient low-complexity iterative receiver for a multiuser MIMO system in time-varying channels, that scales linear in the number of users and the length of the observation vector. At the receiver side, we consider an algorithm performing iterative multiuser detection with parallel interference cancellation (PIC) and time-varying channel estimation jointly. For PIC and channel estimation, soft-symbols are used that are supplied by a soft-input soft-output decoder based on the BCJR algorithm [12]. Channel estimation is performed using LMMSE filtering and can be implemented with low-complexity using the Krylov subspace method.

PIC can be implemented in two basic configurations. In the first configuration, the other users interference is subtracted directly from the received chip vector, thus operating in chip space. A second configuration employs matched filtering first and then subtracts the other users interference, thus operating in user space. This model has been introduced in [13] and allows joint detection of all users. The two PIC configurations are mathematically nearly equivalent if an exact linear MMSE filter is employed. However, when using a low complexity implementation based on the Krylov subspace method, the two setups lead to large complexity differences.

In MIMO CDMA channels, joint antenna detection schemes are shown to outperform individual antenna detection schemes [14]. However, such systems are computationally expensive.

Manuscript received March 2, 2007; revised October 17, 2007. This work is funded by the Vienna Science and Technology Fund (WWTF) in the ftw. project Future Mobile Communications Systems (Math+MIMO). Part of this work has been published at the Seventeenth IEEE International Symposium on Personal, Indoor and Mobile Radio Communications (PIMRC'06), Helsinki, Finland, September 2006.

The authors are with the Forschungzentrum Telekommunikation Wien (ftw.), A-1220 Vienna, Austria (e-mail: dumard@ftw.at; thomas.zemen@ftw.at).

Digital Object Identifier 10.1109/TSP.2007.916133

We develop a method to implement such a receiver with low-complexity.

Contributions of the Paper:

- First, we develop a reduced-rank low-complexity channel estimation method for a time-varying MIMO MU uplink based on the Krylov subspace method.
- Second, we implement a joint antenna detector for an MC-CDMA MIMO receiver, using parallel interference cancelation in *chip space*. This approach does not allow complexity reduction but parallelization of the computations into as many branches as transmit antennas. The latency time can thus be reduced by a factor that is proportional to the number of users in case of a fully loaded system.
- Finally, we develop a new model for joint antenna detection with PIC in *user space*. This approach allows saving more than one order of magnitude of complexity with only minor performance losses.

Notation: We denote by $\boldsymbol{a}$ a column vector with ith element $a[i]$. Similarly, $\boldsymbol{A}$ is a matrix with i,ℓth element $[\boldsymbol{A}]_{i,\ell}$. A diagonal matrix with entries $a[i]$ is denoted $\mathrm{diag}(\boldsymbol{a})$. The $Q\times Q$ identity matrix and $Q\times 1$ zero vector are denoted by $\boldsymbol{I}_Q$ and $\boldsymbol{0}_Q$ respectively. We denote the real and conjugate transpose with $^{\mathrm{T}}$ and $^{\mathrm{H}}$ respectively. The largest (respectively smallest) integer, lower (resp. greater) or equal than $a\in\mathbb{R}$ is represented by $\lfloor a\rfloor$ (resp. $\lceil a\rceil$). The ℓ_2-norm is denoted through $\|\boldsymbol{a}\|$. The expectation of a variable is denoted through $\mathsf{E}\{\cdot\}$. The $N_T(k-1)+t$th elementary vector of size KN_T for $k\in\{1,\ldots,K\}$ and $t\in\{1,\ldots,N_T\}$ is represented by $\boldsymbol{e}_{(k,t)}$.

Organization of the Paper: The Krylov subspace method is briefly recalled and details on the computational complexity are given in Section II. The system model is developed in Section III. The low-complexity implementation of the multiple antenna receiver using the Krylov subspace method is described in Section IV. Simulation results as well as complexity comparison are presented in Section V. Section VI summarizes the main results and concludes this work.

II. Complexity of the Krylov Subspace Methods

The main results of this paper are based on the Krylov subspace method which we shortly recall in this section. The complete description of the algorithm can be found in [4]–[7] and more specifically for our use in [15].

Considering a linear system $\boldsymbol{A}\boldsymbol{x}=\boldsymbol{a}$, where $\boldsymbol{A}$ is a known invertible matrix of size $Q\times Q$ and $\boldsymbol{a}$ a known vector of length Q, the Krylov subspace based algorithms compute iteratively (s increasing) an approximation of the solution $\boldsymbol{x}$, starting from an initial guess $\boldsymbol{x}_0$ and using projections on Krylov subspaces of dimension s. The final step S is referred to as the number of iterations in the algorithm or as the dimension of the Krylov subspace on which we project $\boldsymbol{a}-\boldsymbol{A}\boldsymbol{x}_0$.

Using the algorithm which is recalled in Table I, we can now discuss on the computational complexity using the Krylov subspace method for an LMMSE filter. Let us here define a *flop* as a floating-point operation, as given in [16]. A *flop* is either an addition, substraction, multiplication, division or square root operation in the *real* domain. Thus, one complex multiplication (CM) requires four real multiplications and two additions, leading to 6 flops. Similarly, one complex addition (CA) corresponds to 2 flops.

TABLE I
Krylov Subspace-Based Algorithm for a Hermitian Matrix

	Steps	Complexity in $flops$ using (1)
1	input $\boldsymbol{A}$, $\boldsymbol{a}$, $\boldsymbol{x}_0$, S	$2a(4b-1)$ for $\boldsymbol{a}=\boldsymbol{M}\boldsymbol{v}$
2	$\tilde{\boldsymbol{a}}=\boldsymbol{a}-\boldsymbol{A}\boldsymbol{x}_0$	$16ab+8a+4b$
3	$\boldsymbol{v}_1=\tilde{\boldsymbol{a}}/\|\tilde{\boldsymbol{a}}\|$	$10a-1$
4	$\boldsymbol{u}=\boldsymbol{A}\boldsymbol{v}_1$	$16ab+6a+4b$
5	$\alpha=\boldsymbol{v}_1^{\mathrm{H}}\boldsymbol{u}$	$8a-2$
6	$\boldsymbol{c}_{\mathrm{first}}=\boldsymbol{c}_{\mathrm{last}}=1/\alpha$	1
7	$\boldsymbol{w}=\boldsymbol{u}-\alpha\boldsymbol{v}_1$	$8a$
8	for $s=2,\ldots,S$	
9	$\beta=\|\boldsymbol{w}\|$	$8a-1$
10	$\boldsymbol{v}_s=\boldsymbol{w}/\beta$	$2a$
11	$\boldsymbol{u}=\boldsymbol{A}\boldsymbol{v}_s$	$16ab+6a+4b$
12	$\alpha=\boldsymbol{v}_s^{\mathrm{H}}\boldsymbol{u}$	$8a-2$
13	$\gamma=\alpha-\beta^2\boldsymbol{c}_{\mathrm{last}}[s-1]$	$2a+2$
14	$\boldsymbol{c}=\gamma^{-1}\left[-\beta\boldsymbol{c}_{\mathrm{last}}^{\mathrm{T}},1\right]^{\mathrm{T}}$	$6(s+1)$
15	$\boldsymbol{c}_{\mathrm{first}}=\begin{matrix}\left[\boldsymbol{c}_{\mathrm{first}}^{\mathrm{T}},0\right]^{\mathrm{T}}\\ -c_{\mathrm{last}}[1]^*\beta\boldsymbol{c}\end{matrix}$	$8(s+1)$
16	$\boldsymbol{c}_{\mathrm{last}}=\boldsymbol{c}$	
17	$\boldsymbol{w}=\boldsymbol{u}-\alpha\boldsymbol{v}_s-\beta\boldsymbol{v}_{s-1}$	$8a$
18	end	
19	$\boldsymbol{V}_S=[\boldsymbol{v}_1,\ldots,\boldsymbol{v}_S]$	
20	output $\boldsymbol{x}_S=\|\tilde{\boldsymbol{a}}\|\boldsymbol{V}_S\boldsymbol{c}_{\mathrm{first}}+\boldsymbol{x}_0$	$2a(4S+1)$

The general structure of an LMMSE filter can be written as [17]

$$\boldsymbol{f}=\underbrace{\left(\boldsymbol{D}_1+\boldsymbol{M}\boldsymbol{D}_2\boldsymbol{M}^{\mathrm{H}}\right)}_{\boldsymbol{A}}{}^{-1}\boldsymbol{M}\boldsymbol{v} \tag{1}$$

where $\boldsymbol{M}\in\mathbb{C}^{a\times b}$, $\boldsymbol{v}\in\mathbb{C}^b$, and $\boldsymbol{D}_1\in\mathbb{C}^{a\times a}$ and $\boldsymbol{D}_2\in\mathbb{C}^{b\times b}$ are diagonal.

Computing $\boldsymbol{f}$ in (1) directly requires the following operations:

- computation of $\boldsymbol{A}=\boldsymbol{D}_1+\boldsymbol{M}\boldsymbol{D}_2\boldsymbol{M}^{\mathrm{H}}$, i.e., $ab\mathrm{CM}+a^2(b\mathrm{CM}+(b-1)\mathrm{CA})+a\mathrm{CA}=8a^2b+6ab-2a^2+2a$ flops;
- inversion of $\boldsymbol{A}$, i.e., $(1/3)a(a-1)(8a-1)$ flops (see Appendix A for details);
- computation of $\boldsymbol{A}^{-1}\boldsymbol{a}$ with $\boldsymbol{a}=\boldsymbol{M}\boldsymbol{v}$, i.e., $4a(2a+2b-1)$ flops.

This leads to the approximate computational complexity

$$C^1_{\mathrm{LMMSE}}\approx 8a^2\left(\frac{a}{3}+b\right)\ \text{flops}. \tag{2}$$

Using the Krylov approximation, the main computations required to approximate $\boldsymbol{f}$ are as follows:

- the product $\boldsymbol{A}\boldsymbol{v}_s=\boldsymbol{D}_1\boldsymbol{v}_s+\boldsymbol{M}(\boldsymbol{D}_2(\boldsymbol{M}^{\mathrm{H}}\boldsymbol{v}_s))$ for $s\in\{1,\ldots,S\}$, in lines 4 and 11 of the algorithm in Table I, as well as $\boldsymbol{A}\boldsymbol{x}_0$ on line 2, i.e., $(16ab+6a+4b)(S+1)$ flops;
- two inner products for S steps, in lines 3, 5 and lines 9 and 12, i.e., $2(8a-2)S$ flops.

The computational complexity of each step is detailed in Table I. Adding all these steps, the total computational complexity using the Krylov subspace method becomes after approximation

$$C^1_{\mathrm{K}}\approx(16ab+42a)(S+1)+8ab\ \text{flops}. \tag{3}$$

If $a\geq b$, the computational complexity can be reduced by first applying the matrix inversion lemma [6]

to (1). Detailed computations in Appendix B lead to $\boldsymbol{f} = \boldsymbol{D}_1^{-1}\boldsymbol{M}(\alpha\boldsymbol{I}_b + \boldsymbol{D}_2\boldsymbol{M}^{\mathrm{H}}\boldsymbol{D}_1^{-1}\boldsymbol{M})^{-1}\boldsymbol{v}$. Similar computational complexity expressions as (2) and (3) can be obtained for the new LMMSE filter and its Krylov approximation

$$C_{\mathrm{LMMSE}}^2 \approx 8b^2\left(\frac{b}{3}+a\right) \text{ flops}$$
$$C_{\mathrm{K}}^2 \approx (8ab+14b+12a)(2S+3)+12b \text{ flops.} \quad (4)$$

Finally, we obtain for the general case

$$C_{\mathrm{LMMSE}} \approx 8ab\min\{a,b\} + \frac{8}{3}\min\{a,b\}^3 \text{ flops}$$
$$C_{\mathrm{K}} \approx 8ab(2S+3) + 14(S+1)\min\{3a, 2(a+b)\} \text{ flops.} \quad (5)$$

If a and b are high enough, as it will be the case in our application, the second term in C_{K} might be ignored, leading to $C_{\mathrm{K}} \approx 8ab(2S+3)$.

In this approximation, a and b are interchangeable, so we can set $\min\{a,b\} = a$ without loss of generality. The exact LMMSE filter has a complexity of order $\mathcal{O}(8a^2((a/3)+b))$ and the ratio $\gamma = C_{\mathrm{K}}/C_{\mathrm{LMMSE}}$ is of order

$$\mathcal{O}\left(\frac{2S+3}{a\left(\frac{a}{3b}+1\right)}\right) \leq \mathcal{O}\left(\frac{2S+3}{a}\right). \quad (6)$$

Assuming $S \ll a$, the computational complexity reduction by the Krylov subspace method is substantial.

III. System Model

We consider the uplink of an MC-CDMA system. At the same time $K \geq 1$ users having each $N_T \geq 1$ antennas transmit to a receiver with $N_R \geq 1$ antennas. Hence, we have a MIMO multiuser (MU) system. In this section, we detail the model used for the multiple antenna transmitter and receiver.

A. Multiple Antenna Transmitter

Each user $k \in \{1,\ldots,K\}$ has $N_T \geq 1$ transmit antennas. The MC-CDMA uplink transmission is based on orthogonal frequency division multiplexing (OFDM) with N subcarriers, where N is also the spreading factor. We consider the transmission of N_T data blocks per user, each data block consists of $M-J$ OFDM data symbols and J pilot symbols. From the receiver point of view, the KN_T transmit antennas behave like KN_T independent virtual users. Thus, and for clarity, we will refer to the transmit antenna t of user k as transmit antenna or virtual user (k,t). Each transmit antenna $(k,t) \in \{1,\ldots,K\}\times\{1,\ldots,N_T\}$ transmits symbols $b_{(k,t)}[m]$ with symbol rate $1/T_{\mathrm{S}}$, where m denotes the discrete time index and T_{S} the symbol duration. Each symbol $b_{(k,t)}[m]$ is spread by a random spreading sequence $\boldsymbol{s}_{(k,t)} \in \mathbb{C}^N$ with independent identically distributed elements chosen from the set $\{\pm 1 \pm \mathrm{j}\}/\sqrt{2N}$. The data symbols $b_{(k,t)}[m]$ result from the binary information sequence $\chi_k[m'']$ of length $2(M-J)R_C$ by convolutional encoding with code rate R_C, random interleaving and quadrature phase shift keying (QPSK) modulation with Gray labeling.

Fig. 1. Pilot placement for $J = 60$ pilots among $M = 256$ symbols.

The $M-J$ data symbols are distributed over a block of length M fulfilling

$$b_{(k,t)}[m] \in \{\pm 1 \pm \mathrm{j}\}/\sqrt{2} \quad \text{for} \quad m \notin \mathcal{P}$$
$$b_{(k,t)}[m] = 0 \quad \text{for} \quad m \in \mathcal{P} \quad (7)$$

allowing for pilot symbol insertion. The pilot placement is defined through the index set

$$\mathcal{P} = \left\{ \left\lfloor i\frac{M}{J} + \frac{M}{2J} \right\rfloor | i \in \{0,\ldots,J-1\} \right\}. \quad (8)$$

Fig. 1 gives an illustration of the pilot placement.

We use joint encoding [18], [19] for all N_T antennas of one user: the N_T data blocks of one user are jointly encoded, interleaved and mapped. Then the $N_T(M-J)$ coded symbols are split into N_T coded symbol blocks that are independently spread to be transmitted over their corresponding antenna.

After spreading, the pilot symbols $\boldsymbol{p}_{(k,t)}[m] \in \mathbb{C}^N$ are added

$$\boldsymbol{d}_{(k,t)}[m] = \boldsymbol{s}_{(k,t)}b_{(k,t)}[m] + \boldsymbol{p}_{(k,t)}[m]. \quad (9)$$

For $m \in \mathcal{P}$ and $q \in \{0,\ldots,N-1\}$, the elements $p_{(k,t)}[m,q]$ of the pilot symbol vector $\boldsymbol{p}_{(k,t)}[m]$ are randomly chosen from the QPSK symbol set $\{\pm 1 \pm \mathrm{j}\}/\sqrt{2N}$. Otherwise $\boldsymbol{p}_{(k,t)}[m] = \boldsymbol{0}_N$ for $m \notin \mathcal{P}$.

At each transmit antenna an N-point inverse discrete Fourier transform (DFT) is performed and a cyclic prefix of length G is inserted. A single OFDM symbol together with the cyclic prefix has length $P = N+G$ chips. After parallel to serial conversion the chip stream with chip rate $1/T_{\mathrm{C}} = P/T_{\mathrm{S}}$ is transmitted over a time-varying multipath fading channel with L resolvable paths.

The transmission of KN_T symbols at time instant m is done over K independent $N_T \times N_R$ MIMO channels. These KN_TN_R channels are assumed uncorrelated. Thus, the receiver treats the KN_T antennas in the same way as if they were KN_T independent users having one transmit antenna each.

B. Multiple Antenna Receiver

The iterative receiver performing channel estimation and multiuser detection is shown in Fig. 2. The receiver is equipped with $N_R \geq 1$ receive antennas. At each receive antenna $r \in \{1,\ldots,N_R\}$, the signals of all KN_T transmit antennas add up.

Each of the N_R receivers performs cyclic prefix removal and a DFT on its own received signal. After these two operations,

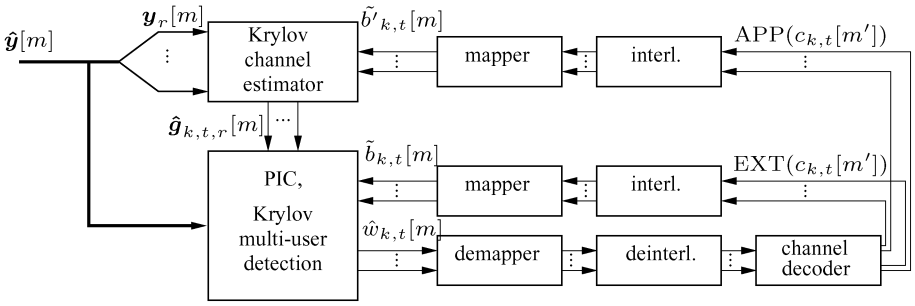

Fig. 2. Iterative MC-CDMA receiver.

the received signal at receive antenna r for subcarrier q and time instant m is given by

$$y_r[m,q] = \sum_{k=1}^{K}\sum_{t=1}^{N_T} g_{(k,t),r}[m,q]d_{(k,t)}[m,q] + z_r[m,q] \quad (10)$$

where $d_{(k,t)}[m,q]$ is the qth element of $\boldsymbol{d}_{(k,t)}[m]$ defined in (9) and complex additive white Gaussian noise with zero mean and covariance σ_z^2 is denoted by $z_r[m,q]$. The time-varying frequency response between transmit antenna (k,t) and receive antenna r for discrete time-index m and subcarrier q is denoted by $g_{(k,t),r}[m,q]$, for $q \in \{0,\ldots,N-1\}, m \in \{0,\ldots,M-1\}$.

In vector notation, (10) becomes

$$\boldsymbol{y}_r[m] = \sum_{k=1}^{K}\sum_{t=1}^{N_T} \mathrm{diag}\left(\boldsymbol{g}_{(k,t),r}[m]\right) \times \left(\boldsymbol{s}_{(k,t)}b_{(k,t)}[m] + \boldsymbol{p}_{(k,t)}[m]\right) + \boldsymbol{z}_r[m] \quad (11)$$

where $\boldsymbol{z}_r[m] = [z_r[m,0],\ldots,z_r[m,N-1]]^{\mathrm{T}}$ and $\boldsymbol{y}_r[m] = [y_r[m,0],\ldots,y_r[m,N-1]]^{\mathrm{T}}$.

All time-varying channels $\boldsymbol{g}_{(k,t),r}$ are assumed uncorrelated. Hence, receive antenna r can perform channel estimation independently from the other receive antennas without loss of information. We define $\hat{\boldsymbol{g}}_{(k,t),r}[m]$ as the channel estimate at discrete time m of the time-varying channel $\boldsymbol{g}_{(k,t),r}$ and the effective spreading sequence for transmit antenna (k,t) at time m as

$$\tilde{\boldsymbol{s}}_{(k,t),r}[m] = \mathrm{diag}\left(\hat{\boldsymbol{g}}_{(k,t),r}[m]\right)\boldsymbol{s}_{(k,t)} \in \mathbb{C}^N. \quad (12)$$

Unless necessary, we will omit the time-index m for clarity sake. The time-varying effective spreading matrix containing the KN_T spreading sequences at receive antenna r is given by

$$\tilde{\boldsymbol{S}}_r = [\underbrace{\tilde{\boldsymbol{s}}_{(1,1),r},\ldots,\tilde{\boldsymbol{s}}_{(1,N_T),r}}_{\text{user 1}},\ldots,\tilde{\boldsymbol{s}}_{(k,t),r},\ldots, \underbrace{\tilde{\boldsymbol{s}}_{(K,1),r},\ldots,\tilde{\boldsymbol{s}}_{(K,N_T),r}}_{\text{user } K}]. \quad (13)$$

Using these definitions the signal received at antenna r given in (11) writes for $m \notin \mathcal{P}$

$$\boldsymbol{y}_r = \tilde{\boldsymbol{S}}_r\boldsymbol{b} + \boldsymbol{z}_r \quad (14)$$

where $\boldsymbol{b}$ contains the data symbols for the KN_T virtual users. To take maximal advantage of the multiantenna structure of the receiver we perform joint antenna detection [14], [19]. Here all N_R received signals are processed jointly. We define

$$\hat{\boldsymbol{y}} = \left[\boldsymbol{y}_1^{\mathrm{T}},\ldots,\boldsymbol{y}_{N_R}^{\mathrm{T}}\right]^{\mathrm{T}} \in \mathbb{C}^{NN_R} \quad (15)$$

containing the N_R received vectors. Similarly, we define the effective spreading matrix

$$\hat{\boldsymbol{S}} = \left[\tilde{\boldsymbol{S}}_1^{\mathrm{T}},\ldots,\tilde{\boldsymbol{S}}_{N_R}^{\mathrm{T}}\right]^{\mathrm{T}} \in \mathbb{C}^{NN_R \mathrm{x} KN_T}. \quad (16)$$

The column $N_T(k-1)+t$ of $\hat{\boldsymbol{S}}$, denoted through $\hat{\boldsymbol{s}}_{(k,t)}$, corresponds to the joint effective spreading sequence of user (k,t) and contains the N_R effective spreading sequences of this user

$$\hat{\boldsymbol{s}}_{(k,t)} = \left[\tilde{\boldsymbol{s}}_{(k,t),1}^{\mathrm{T}},\ldots,\tilde{\boldsymbol{s}}_{(k,t),N_R}^{\mathrm{T}}\right]^{\mathrm{T}}. \quad (17)$$

Similarly, we also define the noise vector with covariance matrix $\sigma_z^2\boldsymbol{I}_{NN_R}$

$$\hat{\boldsymbol{z}} = \left[\boldsymbol{z}_1^{\mathrm{T}},\ldots,\boldsymbol{z}_{N_R}^{\mathrm{T}}\right]^{\mathrm{T}} \in \mathbb{C}^{NN_R}. \quad (18)$$

Using these notations, the joint received vector can be written as

$$\hat{\boldsymbol{y}} = \hat{\boldsymbol{S}}\boldsymbol{b} + \hat{\boldsymbol{z}}. \quad (19)$$

IV. Low Complexity Implementation of the Receiver

The optimal maximum *a posteriori* (MAP) detector [20] for (14) or (19) is prohibitively complex. The MAP detector can be approximated using an iterative linear receiver with parallel interference cancelation (PIC). We perform PIC using the soft symbol estimates $\tilde{b}_{(k,t)}$. These are computed from the extrinsic probabilities supplied by the decoding stage (see Fig. 2)

$$\tilde{b}_{(k,t)}[m] = \frac{1}{\sqrt{2}}\left(2\mathrm{EXT}\left(c_{(k,t)}[2m]\right) - 1\right) + \mathrm{j}\frac{1}{\sqrt{2}}\left(2\mathrm{EXT}\left(c_{(k,t)}[2m+1]\right) - 1\right). \quad (20)$$

We define the error covariance matrix of the soft symbols $\tilde{\boldsymbol{b}}[m] = [\tilde{b}_{(1,1)}[m],\ldots,\tilde{b}_{(k,t)}[m],\ldots,\tilde{b}_{(K,N_T)}[m]]^{\mathrm{T}}$

$$\boldsymbol{V} = \mathsf{E}\left\{(\boldsymbol{b}-\tilde{\boldsymbol{b}})(\boldsymbol{b}-\tilde{\boldsymbol{b}})^{\mathrm{H}}\right\} \quad (21)$$

with constant diagonal elements $[\boldsymbol{V}]_{k,t} = \mathsf{E}\{1 - |\tilde{b}_{(k,t)}|^2\}$. The elements of $\boldsymbol{b}$ and $\tilde{\boldsymbol{b}}$ are supposed to be independent and the off diagonal elements of $\boldsymbol{V}$ are assumed to be zero.

The goal of this paper is to combine the Krylov subspace method with an appropriate iterative receiver structure to minimize the computational complexity. More details follow in Section IV-A for time-varying channel estimation and in Sections IV-B and IV-C for MU-MIMO detection.

A. Iterative Time-Varying Channel Estimation

The performance of the iterative receiver depends on the channel estimates for the time-varying frequency response $\boldsymbol{g}_{(k,t),r}[m]$ since the effective spreading sequence $\tilde{\boldsymbol{s}}_{(k,t),r}$ directly depends on the actual channel realization.

The maximum variation in time of the wireless channel is upper bounded by the maximum normalized one-sided Doppler bandwidth

$$\nu_{\mathrm{Dmax}} = \frac{v_{\max} f_C}{c_0} T_{\mathrm{S}} \tag{22}$$

where $v_{\max}$ is the maximum (supported) velocity, T_{S} is the OFDM symbol duration, f_{C} is the carrier frequency and c_0 the speed of light. Time-limited snapshots of the bandlimited fading process span a subspace with very small dimensionality. The same subspace is spanned by discrete prolate spheroidal (DPS) sequences [21]. The DPS sequences $\{u_i[m]\}$ are defined as [22]

$$\lambda_i u_i[m] = \sum_{\ell=0}^{M-1} \frac{\sin\left(2\pi\nu_{\mathrm{Dmax}}(\ell - m)\right)}{\pi(\ell - m)} u_i[\ell]. \tag{23}$$

The sequences $\{u_i[m]\}$ are doubly orthogonal over the infinite set $\{-\infty, \ldots, \infty\}$ and the finite set $\mathcal{I}_M = \{0, \ldots, M-1\}$, bandlimited by ν_{Dmax} and maximally energy concentrated on $\mathcal{I}_M$.

We are interested in describing the time-varying frequency selective channel $\boldsymbol{g}_{r,(k,t)}$ for the duration of a single data block $\mathcal{I}_M$. For $m \in \mathcal{I}_M$, we model the time-varying channel $\boldsymbol{g}_{r,(k,t)}[m]$ using the Slepian basis expansion [21]. The Slepian basis functions $\boldsymbol{u}_i = [u_i[0], \ldots, u_i[M-1]]^{\mathrm{T}}$ for $i \in \{0, \ldots, D-1\}$ are the time-limited DPS sequences. The eigenvalue λ_i are ordered such that $\lambda_1 > \lambda_2 \ldots > \lambda_M$.

The time-varying channel $\boldsymbol{g}_{r,(k,t)}[m] \in \mathbb{C}^N$ is projected onto the subspace spanned by the first D Slepian sequences and is approximated as

$$g_{(k,t),r}[m,q] \approx \tilde{g}_{(k,t),r}[m,q] = \sum_{i=0}^{D-1} u_i[m]\psi_{(k,t),r}[i,q] \tag{24}$$

for $m \in \mathcal{I}_M$ and $q \in \{0, \ldots, N-1\}$. The dimension D of this basis expansion fulfills $\lceil 2\nu_{\mathrm{Dmax}} M \rceil + 1 \leq D \ll M - 1$. For practical mobile communication systems, $D \leq 5$ for $M = 256$, see [21]. Substituting the basis expansion (24) for the time-varying subcarrier coefficients $g_{(k,t),r}[m,q]$ into the system model (10) we obtain

$$y_r[m,q] = \sum_{k=1}^{K}\sum_{t=1}^{N_T}\sum_{i=0}^{D-1} u_i[m]\psi_{(k,t),r}[i,q]d_{(k,t)}[m,q] + z_r[m,q] \tag{25}$$

where $d_{(k,t)}[m,q]$ are the elements of $\boldsymbol{d}_{(k,t)}[m]$ defined in (9).

For channel estimation, J pilot symbols in (9) are known. The remaining $M - J$ symbols are not known. We replace them by soft symbols that are calculated from the *a posteriori* probabilities (APP) obtained in the previous iteration from the BCJR decoder output. The soft symbols are computed as

$$\tilde{b}'_{(k,t)}[m] = \frac{1}{\sqrt{2}}\left(2\mathrm{APP}\left(c_{(k,t)}[2m]\right) - 1\right) + \mathrm{j}\frac{1}{\sqrt{2}}\left(2\mathrm{APP}\left(c_{(k,t)}[2m+1]\right) - 1\right). \tag{26}$$

This enables us to obtain refined channel estimates if the soft symbols get more reliable from iteration to iteration.

The KN_TN_R channels are assumed uncorrelated, thus channel estimation can be performed for every receive antenna independently, without loss of information. For clarity, we drop the subscript r in the following.

At each receive antenna, the subcarrier coefficients $\psi_{(k,t)}[i,q]$ can be obtained jointly for all KN_T virtual users but individually for every subcarrier q. We define the vectors

$$\boldsymbol{\psi}_{q,d} = \left[\psi_{(1,1)}[d,q], \ldots, \psi_{(1,N_T)}[d,q], \ldots, \psi_{(K,1)}[d,q], \ldots, \psi_{(K,N_T)}[d,q]\right]^{\mathrm{T}} \in \mathbb{C}^{KN_T} \tag{27}$$

for $d \in \{0, \ldots, D-1\}$ and

$$\boldsymbol{\phi}_q = \left[\boldsymbol{\psi}_{q,0}^{\mathrm{T}}, \ldots, \boldsymbol{\psi}_{q,D-1}^{\mathrm{T}}\right]^{\mathrm{T}} \in \mathbb{C}^{KN_TD} \tag{28}$$

containing the basis expansion coefficients of all KN_T virtual users for subcarrier q. The received symbol sequence of each single data block on subcarrier q is given by

$$\boldsymbol{y}_q = [y[0,q], \ldots, y[M-1,q]]^{\mathrm{T}} \in \mathbb{C}^M. \tag{29}$$

Using these definitions we write

$$\boldsymbol{y}_q = \tilde{\boldsymbol{\mathcal{D}}}_q\boldsymbol{\phi}_q + \boldsymbol{z}_q \tag{30}$$

where

$$\tilde{\boldsymbol{\mathcal{D}}}_q = \left[\mathrm{diag}(\boldsymbol{u}_0)\tilde{\boldsymbol{D}}_q, \ldots, \mathrm{diag}(\boldsymbol{u}_{D-1})\tilde{\boldsymbol{D}}_q\right] \in \mathbb{C}^{M \times KN_TD}. \tag{31}$$

The matrix $\tilde{\boldsymbol{D}}_q \in \mathbb{C}^{M \times KN_T}$ contains all the transmitted symbols at all time instants $m \in \mathcal{I}_M$ on subcarrier q

$$\tilde{\boldsymbol{D}}_q = \begin{bmatrix} \tilde{d}'_{(1,1)}[0,q] & \cdots & \tilde{d}'_{(K,N_T)}[0,q] \\ \vdots & \ddots & \vdots \\ \tilde{d}'_{(1,1)}[M-1,q] & \cdots & \tilde{d}'_{(K,N_T)}[M-1,q] \end{bmatrix} \tag{32}$$

Here, $\tilde{d}'_{(k,t)}[m,q] = s_{(k,t)}[q]\tilde{b}'_{(k,t)}[m] + p_{(k,t)}[m,q]$ are computed using the APP provided by the decoding stage (26).

The LMMSE estimator can be expressed as [1]–[3]

$$\hat{\boldsymbol{\phi}}_q = \left(\tilde{\boldsymbol{\mathcal{D}}}_q^{\mathrm{H}}\boldsymbol{\Delta}^{-1}\tilde{\boldsymbol{\mathcal{D}}}_q + \boldsymbol{\mathcal{C}}_\phi^{-1}\right)^{-1}\tilde{\boldsymbol{\mathcal{D}}}_q^{\mathrm{H}}\boldsymbol{\Delta}^{-1}\boldsymbol{y}_q. \tag{33}$$

where $\boldsymbol{\Delta} \triangleq \boldsymbol{\Lambda} + \sigma_z^2\boldsymbol{I}_M \in \mathbb{C}^{M \times M}$ and the elements of the diagonal matrix $\boldsymbol{\Lambda} \in \mathbb{C}^{M \times M}$ are defined as

$$\boldsymbol{\Lambda}_{mm} = \frac{1}{\nu_{\mathrm{Dmax}}}\sum_{k=1}^{K}\sum_{t=1}^{N_T}\sum_{i=0}^{D-1}\frac{1}{N}\lambda_i u_i^2[m]\left(1 - \left|\tilde{b}'_{(k,t)}[m]\right|^2\right). \tag{34}$$

The diagonal covariance matrix $\boldsymbol{\mathcal{C}}_\phi$ for $\boldsymbol{\phi_q}$ is given by

$$\boldsymbol{\mathcal{C}}_\phi = \frac{1}{2\nu_{\mathrm{Dmax}}}\mathrm{diag}\left([\lambda_0, \ldots, \lambda_{D-1}]\right) \otimes \boldsymbol{I}_{KN_T} \tag{35}$$

where $\otimes$ denotes the Kronecker matrix product. We note that $\boldsymbol{C}_\phi$ does not depend on the subcarrier q.

After estimating $\boldsymbol{\phi}_q$ and using (27) and (28), an estimate for the time-varying frequency response is given by

$$\hat{g}'_{(k,t)}[m,q] = \sum_{i=0}^{D-1} u_i[m]\hat{\psi}_{(k,t)}[i,q]. \tag{36}$$

Further noise suppression is achieved if we exploit the correlation between the subcarriers

$$\hat{\boldsymbol{g}}_{(k,t)}[m] = \boldsymbol{F}_{N\times L}\boldsymbol{F}^{\mathrm{H}}_{N\times L}\hat{\boldsymbol{g}}'_{(k,t)}[m], \tag{37}$$

where $[\boldsymbol{F}_{N\times L}]_{i,\ell} = 1/\sqrt{N}\mathrm{e}^{-\mathrm{j}2\pi i\ell/N}$ for $(i,\ell) \in \{0,\ldots,N-1\}\times\{0,\ldots,L-1\}$.

For the projection (37), a different set of DPS sequences could be used as well in the frequency domain [23]. However, using DPS sequences in the frequency domain leads to a small reduction in BER only. Hence, we choose the low complexity DFT implementation.

Given $\boldsymbol{D}_1 = \boldsymbol{C}_\phi$, $\boldsymbol{D}_2 = \boldsymbol{\Delta}^{-1}$, $\boldsymbol{M} = \tilde{\boldsymbol{\mathcal{D}}}_q^{\mathrm{H}}$, $\boldsymbol{v} = \boldsymbol{\Delta}^{-1}\boldsymbol{y}$, $a = KN_TD$ and $b = M$, we can use the model in Section II. With the parameters used in our simulations, $b \le a$. Here the approximation is computed individually for each subcarrier q but jointly for all virtual users (k,t). We are able to use the results (5) for the computational complexity. Channel estimation is done at each receive antenna, thus a factor N_R appears, leading to the expressions of the complexity per subcarrier

$$\begin{aligned} C_{\mathrm{LMMSE}} &\approx 8N_RM^2\left(\frac{M}{3} + KN_TD\right) \\ C_{\mathrm{K}} &\approx 8MKN_TDN_R(2S+3). \end{aligned} \tag{38}$$

The ratio $\gamma = C_{\mathrm{K}}/C_{\mathrm{LMMSE}}$ is of order $\mathcal{O}(2(S+3)/M)$. Depending on the Krylov subspace dimension S, considerable computational complexity reduction can be achieved.

B. PIC in Chip Space

In this section, we briefly recall iterative multiuser detection based on PIC in chip space [2], [19] and describe its implementation using the Krylov subspace method. After parallel interference cancelation for user (k,t), the received signal (19) becomes

$$\begin{aligned} \breve{\boldsymbol{y}}_{(k,t)} &= \hat{\boldsymbol{y}} - \hat{\boldsymbol{S}}\tilde{\boldsymbol{b}} + \hat{\boldsymbol{s}}_{(k,t)}\tilde{b}_{(k,t)} \\ &= \hat{\boldsymbol{S}}(\boldsymbol{b}-\tilde{\boldsymbol{b}}) + \hat{\boldsymbol{s}}_{(k,t)}\tilde{b}_{(k,t)} + \hat{\boldsymbol{z}}. \end{aligned} \tag{39}$$

The corresponding unbiased LMMSE filter [17] is

$$\hat{\boldsymbol{f}}^{\mathrm{H}}_{(k,t)} = \frac{\hat{\boldsymbol{s}}^{\mathrm{H}}_{(k,t)}\left(\sigma_z^2\boldsymbol{I}_{NN_R} + \hat{\boldsymbol{S}}\boldsymbol{V}\hat{\boldsymbol{S}}^{\mathrm{H}}\right)^{-1}}{\hat{\boldsymbol{s}}^{\mathrm{H}}_{(k,t)}\left(\sigma_z^2\boldsymbol{I}_{NN_R} + \hat{\boldsymbol{S}}\boldsymbol{V}\hat{\boldsymbol{S}}^{\mathrm{H}}\right)^{-1}\hat{\boldsymbol{s}}_{(k,t)}} \tag{40}$$

and the estimate of $b_{(k,t)}$ is given by $\hat{w}_{(k,t)} = \hat{\boldsymbol{f}}^{\mathrm{H}}_{(k,t)}\breve{\boldsymbol{y}}_{(k,t)}$. These KN_TM estimates are then demapped, deinterleaved and decoded using a BCJR decoder [12].

Given $\boldsymbol{D}_1 = \sigma_z^2\boldsymbol{I}_{NN_R}$, $\boldsymbol{D}_2 = \boldsymbol{V}$, $\boldsymbol{M} = \hat{\boldsymbol{S}}$, $\boldsymbol{v} = \boldsymbol{e}_{(k,t)}$, $a = NN_R$ and $b = KN_T$, we can use the model in Section II to obtain expressions for the computational complexity. We assume a non overloaded system, thus $b \le a$. In this situation, each virtual user (k,t) requires its own filter, while the KN_T filters (40) have a common matrix inverse. However, an approximation algorithm such as the Krylov subspace method has to be performed *per (virtual) user*. This adds a multiplicative factor KN_T in the global computational complexity using the Krylov subspace method, leading to

$$\begin{aligned} C_{\mathrm{LMMSE}} &\approx 8(KN_T)^2\left(NN_R + \frac{KN_T}{3}\right) \\ C_{\mathrm{K}} &\approx 8NN_R(KN_T)^2(2S+3). \end{aligned} \tag{41}$$

For a nonoverloaded system (i.e., $KN_T \le NN_R$), the ratio

$$\gamma = \frac{C_{\mathrm{K}}}{C_{\mathrm{LMMSE}}} = \frac{2S+3}{1+\frac{KN_T}{3NN_R}} \tag{42}$$

satisfies $3/4(2S+3) \le \gamma \le 2S+3$. Thus, γ is of order $\mathcal{O}(2S+3)$. The complexity reduction expected by using the Krylov subspace method is neutralized by the multiplicative factor KN_T and no computational complexity is achieved. However parallelization of the computations in KN_T branches is possible [19], allowing dividing latency time by a factor $KN_T/(2S+3)$.

C. PIC in User Space

We want to define an LMMSE filter that allows joint detection of all users using only one filter in order to solve the complexity problem mentioned above in Section IV-B.

We apply a matched filter on the received signal (19), without loss of information [20]

$$\boldsymbol{x} = \hat{\boldsymbol{S}}^{\mathrm{H}}\hat{\boldsymbol{y}} = \hat{\boldsymbol{S}}^{\mathrm{H}}\hat{\boldsymbol{S}}\boldsymbol{b} + \hat{\boldsymbol{S}}^{\mathrm{H}}\hat{\boldsymbol{z}}. \tag{43}$$

Performing interference cancelation for user (k,t) in a mathematically exactly identical way as in (39) writes

$$\hat{\boldsymbol{x}}_{(k,t)} = \hat{\boldsymbol{S}}^{\mathrm{H}}\hat{\boldsymbol{y}} - \hat{\boldsymbol{S}}^{\mathrm{H}}\hat{\boldsymbol{S}}\tilde{\boldsymbol{b}} + \hat{\boldsymbol{S}}^{\mathrm{H}}\hat{\boldsymbol{s}}_{(k,t)}\tilde{b}_{(k,t)}. \tag{44}$$

In this equation, the element $\hat{x}_{(k,t)} = \boldsymbol{e}^{\mathrm{T}}_{(k,t)}\hat{\boldsymbol{x}}_{(k,t)}$ contains most information on the specific user (k,t). In all other elements of $\hat{\boldsymbol{x}}_{(k,t)}$, the information about user (k,t) consists of interference which is mostly canceled using PIC. From now on, we set these correcting terms to zero. This way the received signal after PIC for user (k,t) becomes

$$\hat{x}_{(k,t)} = x_{(k,t)} - \hat{\boldsymbol{s}}^{\mathrm{H}}_{(k,t)}\hat{\boldsymbol{S}}\tilde{\boldsymbol{b}} + \hat{\boldsymbol{s}}^{\mathrm{H}}_{(k,t)}\hat{\boldsymbol{s}}_{(k,t)}\tilde{b}_{(k,t)}. \tag{45}$$

Combining these KN_T expressions in a matrix form leads to

$$\hat{\boldsymbol{x}} = \hat{\boldsymbol{S}}^{\mathrm{H}}\hat{\boldsymbol{y}} - (\hat{\boldsymbol{S}}^{\mathrm{H}}\hat{\boldsymbol{S}} - \hat{\boldsymbol{D}})\tilde{\boldsymbol{b}} \tag{46}$$

where $\hat{\boldsymbol{D}} \in \mathbb{C}^{KN_T\times KN_T}$ is defined as the diagonal matrix with diagonal elements of the covariance matrix $\hat{\boldsymbol{R}} = \hat{\boldsymbol{S}}^{\mathrm{H}}\hat{\boldsymbol{S}}$, $[\hat{\boldsymbol{D}}]_{i,i} = [\hat{\boldsymbol{R}}]_{i,i}$ for $i \in \{1,\ldots,KN_T\}$.

Performing PIC in user space as described in (46) allows joint detection of all users *using one filter only*. It is expected that some information will get lost since we have set some terms to zero, and as a consequence performance will slightly degrade.

The LMMSE filter for PIC in user space $\hat{\boldsymbol{F}}$ defined by $\hat{\boldsymbol{F}}^{\mathrm{H}} = \arg\min_{F} \mathsf{E}\{||\boldsymbol{F}^{\mathrm{H}}\hat{\boldsymbol{x}} - \boldsymbol{b}||^2\}$ can be expressed as

$$\hat{\boldsymbol{F}}^{\mathrm{H}} = (\boldsymbol{V}\hat{\boldsymbol{R}} - \boldsymbol{V}\hat{\boldsymbol{D}} + \hat{\boldsymbol{D}}) \left(\hat{\boldsymbol{R}}\boldsymbol{V}\hat{\boldsymbol{R}} + \sigma_z^2\hat{\boldsymbol{R}} + \hat{\boldsymbol{D}}(\boldsymbol{I}_{KN_T} - \boldsymbol{V})\hat{\boldsymbol{D}}\right)^{-1}. \tag{47}$$

The proof of (47) can be found in Appendix C. Estimates $\hat{w}_{(k,t)}$ of the transmitted symbols $b_{(k,t)}$ are then given in $\hat{\boldsymbol{w}} = \hat{\boldsymbol{F}}^{\mathrm{H}}\hat{\boldsymbol{x}}$. The KN_TM estimates are demapped, deinterleaved and decoded by a BCJR decoder.

Although the LMMSE filter in this case is more complex than the one in chip space, the product $\boldsymbol{F}^{\mathrm{H}}\hat{\boldsymbol{x}}$ needs to be computed only once to detect all users simultaneously. Thus, the use of the Krylov subspace method allows a considerable computational complexity reduction, as we will show now.

Applying the Krylov method to the LMMSE filter (47), we need to define

$$\begin{aligned} \boldsymbol{A} &= \hat{\boldsymbol{R}}\boldsymbol{V}\hat{\boldsymbol{R}} + \sigma_z^2\hat{\boldsymbol{R}} + \hat{\boldsymbol{D}}(\boldsymbol{I}_{KN_T} - \boldsymbol{V})\hat{\boldsymbol{D}} \in \mathbb{C}^{KN_T \times KN_T}, \\ \boldsymbol{a} &= \hat{\boldsymbol{x}} = \hat{\boldsymbol{S}}^{\mathrm{H}}\hat{\boldsymbol{y}} - (\hat{\boldsymbol{S}}^{\mathrm{H}}\hat{\boldsymbol{S}} - \hat{\boldsymbol{D}})\tilde{\boldsymbol{b}} \in \mathbb{C}^{KN_T}. \end{aligned} \tag{48}$$

In this case $\boldsymbol{A}$ slightly differs from the model in Section II. However, replacing the complexity of the computation of $\boldsymbol{a}$, $\boldsymbol{A}$ and the multiplication of $\boldsymbol{A}$ with a vector, the following expressions are obtained

$$\begin{aligned} C_{\mathrm{LMMSE}} &\approx 8(KN_T)^2\left(NN_R + \frac{4}{3}KN_T\right) \\ C_{\mathrm{K}} &\approx 48KNN_TN_RS + 72KNN_RN_T. \end{aligned} \tag{49}$$

Note that in this case, no simple expression can be obtained for the filter (47) using a matrix inversion lemma, thus an eventual computational complexity reduction can not be achieved this way. Assuming KN_T and NN_R are of the same order, (49) cannot be simplified in an obvious manner. However the ratio

$$\gamma = \frac{C_{\mathrm{K}}}{C_{\mathrm{LMMSE}}} = \frac{6S+9}{KN_T\left(1 + \frac{4KN_T}{3NN_R}\right)} \tag{50}$$

is of order $\mathcal{O}((6S+9)/KN_T)$. Hence, and depending on the Krylov subspace dimension S, considerable computational complexity reduction can be achieved.

V. Simulation Results

A. Simulation Setup

We use the same simulation setup as in [1], [2]. The realizations of the time-varying frequency-selective channel $h_{(k,t),r}[n,\ell]$, sampled at the chip rate $1/T_{\mathrm{C}}$, are generated using an exponentially decaying power delay profile

$$\eta^2[\ell] = \mathrm{e}^{-\frac{\ell}{4}} / \sum_{\ell'=0}^{L-1} \mathrm{e}^{-\frac{\ell'}{4}} \tag{51}$$

with root mean-square delay spread $T_{\mathrm{D}} = 4T_{\mathrm{C}} = 1\ \mu$s for a chip rate of $1/T_{\mathrm{C}} = 3.84 \cdot 10^6\ \mathrm{s}^{-1}$ [24]. We assume $L = 15$ resolvable paths. The autocorrelation for every channel tap is given by the classical Clarke spectrum [25]. The system operates at carrier frequency $f_C = 2$ GHz and $K = 32$ users move with velocity $v = 70\ \mathrm{kmh}^{-1}$. These gives a Doppler bandwidth of $B_{\mathrm{D}} = 126$ Hz. We use $N_T = 4$ transmit antennas per user and $N_R = 4$ receive antennas at the base station. The number of subcarriers is $N = 64$ and the OFDM symbol with cyclic prefix has length $P = G + N = 79$. The data block consists of $M = 256$ OFDM symbols including $J = 60$ pilot symbols. The system is designed for $v_{\max} = 102.5\ \mathrm{kmh}^{-1}$ which results in a dimension $D = 3$ for the Slepian basis expansion. The MIMO channel taps are normalized so that

$$\mathsf{E}\left\{\sum_{r=1}^{N_R}\sum_{t=1}^{N_T}\sum_{\ell=0}^{L-1}|h_{(k,t),r}[n,\ell]|^2\right\} = 1 \tag{52}$$

in order to analyze the diversity gain of the receiver only. No antenna gain is present due to this normalization.

For data transmission, a convolutional, nonsystematic, nonrecursive, four state, rate $R_C = 1/2$ code with code generators [101] and [111], see [26], denoted in octal notation $(5,7)_8$, is used. All illustrated results are obtained by averaging over 100 independent channel realizations. The QPSK symbol energy is normalized to 1 and we define the signal-to-noise ratio (SNR)

$$E_b/N_0 = \frac{1}{2R_C\sigma_z^2}\frac{P}{N}\frac{M}{M-J} \tag{53}$$

taking into account the loss due to coding, pilots and cyclic prefix. The noise variance σ_z^2 is assumed to be known at the receiver.

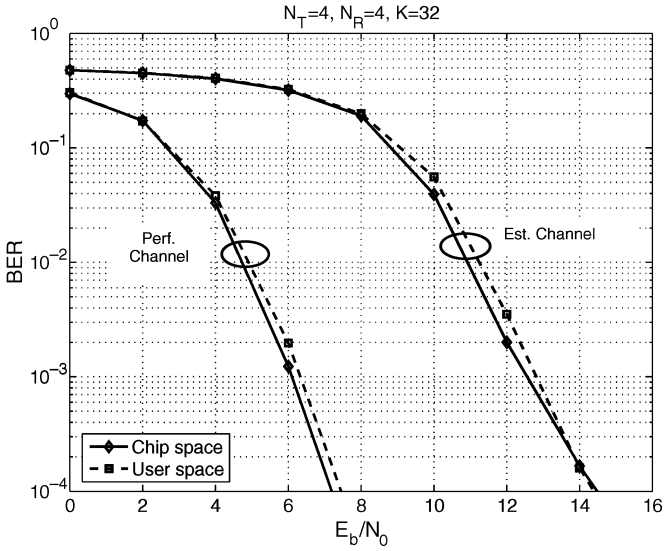

Fig. 3. **Detection Methods Comparison:** BER versus SNR after receiver iteration 4 for $K = 32$ users. We compare the performance of joint antenna detection with PIC in chip space (denoted "Chip") and in user space (denoted "User").

B. Discussion of the Results

Simulations are performed in three steps. Firstly, we compare PIC in chip and in user space in terms of bit-error-rate (BER) versus SNR. All filters are exact LMMSE filters, and the receiver performs four iterations. In Fig. 3, we see that when PIC is performed in the user space, a slight increase in BER can be observed.

Second, we focus on the joint antenna detector with PIC in user space: at this point, the channel is either assumed to be perfectly known or that LMMSE channel estimates are used. The multiuser detector utilizes the Krylov subspace method.

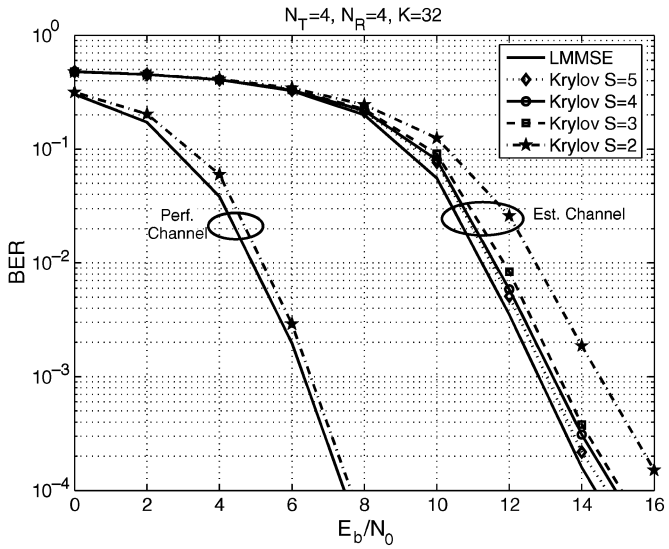

Fig. 4. **Performance of the Krylov subspace method for joint antenna detection with PIC in user space:** BER versus SNR after receiver iteration 4 for $K = 32$ users. The channel is either assumed perfectly known at the receiver or we use LMMSE estimates. We vary the Krylov subspace dimension S for multiuser detection.

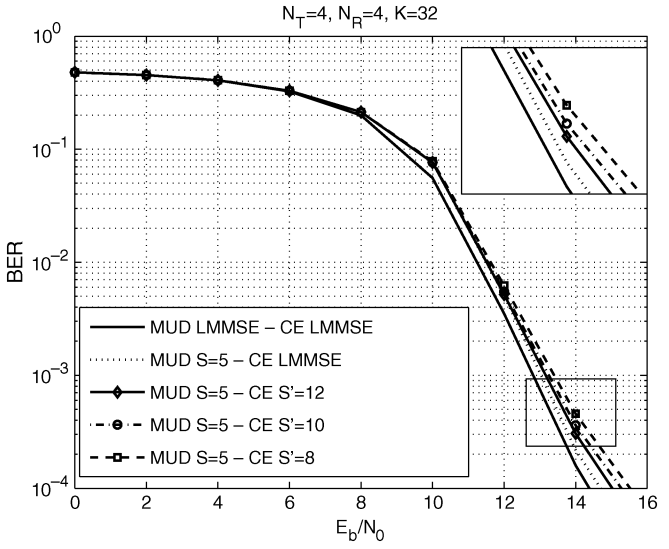

Fig. 5. **Performance of the double Krylov subspace method:** BER versus SNR after receiver iteration 4 for $K = 32$ users. Joint antenna detection is performed after PIC in user space. Both multiuser detection (MUD) and channel estimation (CE) are performed using the Krylov subspace method, and we vary the Krylov subspace dimension S' for channel estimation. For multiuser detection, $S = 5$ is kept constant.

Fig. 4 shows the BER curves for varying Krylov subspace dimension S. As lower bound we plot the BER curve with the exact LMMSE filter for multiuser detection. When the channel is perfectly known, $S = 2$ is sufficient to reach LMMSE multiuser detection performance. When LMMSE channel estimates are used, some loss in performance appears, and a higher subspace dimension is required ($S = 5$ leads to a loss of approximatively 0.25 dB). The expected computational complexity reduction involved allows trading accuracy for efficiency.

At the final step, we keep $S = 5$ constant for joint antenna detection with PIC in user space, and vary the Krylov subspace dimension S' for channel estimation. Results are shown in Fig. 5. Again, a slight loss is inevitable but a trade-off has to be made between computation complexity and performance. A dimension $S' = 12$ is sufficient for channel estimation, introducing a loss of about 0.5 dB compared to the double LMMSE receiver.

Knowing these results, we now compare the computational complexity quantities. We plot the computational complexity in Fig. 6 for $S = 5$, $S' = 12$ as obtained from the simulations. Exact LMMSE computation and its approximation using the Krylov subspace method are compared.

The following observations can be made from these results.

- The use of the Krylov subspace method for channel estimation with $S' = 12$ allows a complexity reduction of about one order of magnitude.
- For PIC in chip space, the use of the Krylov approximation induces an increase in complexity of about one order of magnitude. However, it allows parallelization of the computations in KN_T branches, reducing processing delay with a factor $KN_T/(2S + 3) \approx 19, 7$.
- Using PIC in user space allows joint detection of all users using only one filter. Applying the Krylov subspace method leads to computational complexity reduction by more than one order of magnitude for multiuser detection.

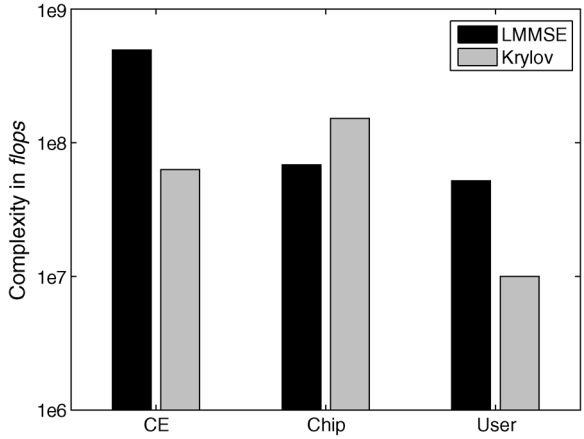

Fig. 6. Computational complexity: We show Krylov (left) and LMMSE (right) implementations, per receiver iteration. Parameters are $S' = 12$ for channel estimation (denoted "CE"), $S = 5$ for multiuser detection using joint antenna detection with PIC in chip space (denoted "Chip") or in user space (denoted "User"). $K = 32$, $N_T = N_R = 4$, $M = 256$, $J = 60$ and $D = 3$.

This complexity reduction comes at the cost of a slight increase of BER (about 0.5 dB).

VI. Conclusion

We have presented a low-complexity receiver performing joint antenna detection. Trading accuracy for efficiency, we approximate the two LMMSE filters for joint time-varying channel estimation and multiuser detection using the Krylov subspace method. Combined with interference cancelation in the user space, our new method allows drastic computational complexity reduction of one order of magnitude at the channel estimator as well as at the multiuser detector, compared to a system using exact LMMSE filters. Using the Krylov subspace

TABLE II
GAUSSIAN ELIMINATION FOR $\boldsymbol{A}$ OF SIZE $Q \times Q$

1	for $q = 1 : Q-1$
2	$\boldsymbol{A}(q+1:Q, q) = \boldsymbol{A}(q+1:Q)/[\boldsymbol{A}]_{q,q}$
3	$\boldsymbol{A}(q+1:Q, q+1:Q) = \boldsymbol{A}(q+1:Q, q+1:Q) - \boldsymbol{A}(q+1:Q)\boldsymbol{A}(Q, q+1)$
4	end

methods implies a slight loss in performance which is negligible compared to the gain in computational complexity.

APPENDIX A
INVERSION OF A COMPLEX MATRIX USING GAUSSIAN ELIMINATION [16]

The Gaussian elimination algorithm [16] to invert a matrix $\boldsymbol{A}$ of size $Q \times Q$ is given in Table II.

For each step q, $Q-q$ multiplications are needed at line 2 and $(Q-q)^2$ multiplications as well as $(Q-q)^2$ additions at line 3. This leads to the total computational complexity in a complex case (recalling one complex multiplication corresponds to 6 flops and one complex addition requires 2 flops):

$$\begin{aligned} C_{\mathrm{GE}} &= \sum_{q=1}^{Q-1} \left(2(Q-q) + 8(Q-q)^2\right) \\ &= \sum_{q=1}^{Q-1} (2q + 8q^2) \\ &= \frac{1}{3} Q(Q-1)(8Q-1). \end{aligned} \tag{54}$$

APPENDIX B
MATRIX INVERSION LEMMA FOR EQUATION (1)

Using the matrix inversion lemma in [6], we can write

$$\begin{aligned} (\boldsymbol{D}_1 + \boldsymbol{M}\boldsymbol{D}_2\boldsymbol{M}^{\mathrm{H}})^{-1} &= \boldsymbol{D}_1^{-1} - \boldsymbol{D}_1^{-1}\boldsymbol{M} \\ &\quad \times \left(\boldsymbol{D}_2^{-1} + \boldsymbol{M}^{\mathrm{H}}\boldsymbol{D}_1^{-1}\boldsymbol{M}\right)^{-1} \boldsymbol{M}^{\mathrm{H}}\boldsymbol{D}_1^{-1} \end{aligned} \tag{55}$$

leading to

$$\begin{aligned} &(\boldsymbol{D}_1 + \boldsymbol{M}\boldsymbol{D}_2\boldsymbol{M}^{\mathrm{H}})^{-1}\boldsymbol{M} \\ &\quad = \boldsymbol{D}_1^{-1}\boldsymbol{M} - \boldsymbol{D}_1^{-1}\boldsymbol{M}\left(\boldsymbol{D}_2^{-1} + \boldsymbol{M}^{\mathrm{H}}\boldsymbol{D}_1^{-1}\boldsymbol{M}\right)^{-1}\boldsymbol{M}^{\mathrm{H}}\boldsymbol{D}_1^{-1}\boldsymbol{M} \\ &\quad = \boldsymbol{D}_1^{-1}\boldsymbol{M}\left(\boldsymbol{I}_b - \left(\boldsymbol{D}_2^{-1} + \boldsymbol{M}^{\mathrm{H}}\boldsymbol{D}_1^{-1}\boldsymbol{M}\right)^{-1}\boldsymbol{M}^{\mathrm{H}}\boldsymbol{D}_1^{-1}\boldsymbol{M}\right) \\ &\quad = \boldsymbol{D}_1^{-1}\boldsymbol{M}\left(\boldsymbol{D}_2^{-1} + \boldsymbol{M}^{\mathrm{H}}\boldsymbol{D}_1^{-1}\boldsymbol{M}\right)^{-1}\boldsymbol{D}_2^{-1} \\ &\quad = \boldsymbol{D}_1^{-1}\boldsymbol{M}\left(\boldsymbol{I}_b + \boldsymbol{D}_2\boldsymbol{M}^{\mathrm{H}}\boldsymbol{D}_1^{-1}\boldsymbol{M}\right)^{-1}. \end{aligned} \tag{56}$$

Finally, we obtain

$$(\boldsymbol{D}_1 + \boldsymbol{M}\boldsymbol{D}_2\boldsymbol{M}^{\mathrm{H}})^{-1}\boldsymbol{M} = \boldsymbol{D}_1^{-1}\boldsymbol{M}\left(\boldsymbol{I}_b + \boldsymbol{D}_2\boldsymbol{M}^{\mathrm{H}}\boldsymbol{D}_1^{-1}\boldsymbol{M}\right)^{-1}. \tag{57}$$

APPENDIX C
DERIVATION OF THE LMMSE FILTER (47)

We need to determine $\hat{\boldsymbol{F}}$ such as

$$\hat{\boldsymbol{F}}^{\mathrm{H}} = \arg\min_{\hat{\boldsymbol{F}}} \mathsf{E}\left\{\|\hat{\boldsymbol{F}}^{\mathrm{H}}\hat{\boldsymbol{x}} - \boldsymbol{b}\|^2\right\} \tag{58}$$

where $\hat{\boldsymbol{x}} = \tilde{\boldsymbol{S}}^{\mathrm{H}}\hat{\boldsymbol{y}} - (\hat{\boldsymbol{S}}^{\mathrm{H}}\hat{\boldsymbol{S}} - \hat{\boldsymbol{D}})\tilde{\boldsymbol{b}}$. We can write

$$\begin{aligned} &\|\hat{\boldsymbol{F}}^{\mathrm{H}}\hat{\boldsymbol{x}} - \boldsymbol{b}\|^2 \\ &\quad = \mathrm{tr}\left\{(\hat{\boldsymbol{F}}^{\mathrm{H}}\hat{\boldsymbol{x}} - \boldsymbol{b})(\hat{\boldsymbol{x}}^{\mathrm{H}}\hat{\boldsymbol{F}} - \boldsymbol{b}^{\mathrm{H}})\right\} \\ &\quad = \mathrm{tr}\left\{\underbrace{\hat{\boldsymbol{F}}^{\mathrm{H}}\hat{\boldsymbol{x}}\hat{\boldsymbol{x}}^{\mathrm{H}}\hat{\boldsymbol{F}}}_{(a)} - \underbrace{\boldsymbol{b}\hat{\boldsymbol{x}}^{\mathrm{H}}\hat{\boldsymbol{F}}}_{(b)} - \underbrace{\hat{\boldsymbol{F}}^{\mathrm{H}}\hat{\boldsymbol{x}}\boldsymbol{b}^{\mathrm{H}}}_{(b)^{\mathrm{H}}} + \underbrace{\boldsymbol{b}\boldsymbol{b}^{\mathrm{H}}}_{(c)}\right\} \end{aligned} \tag{59}$$

where $\mathrm{tr}\{\cdot\}$ designs the trace of a matrix. We analyze separately the elements (a), (b), and (c) of the previous equation. We recall that $\mathsf{E}\{\tilde{\boldsymbol{b}}\boldsymbol{b}^{\mathrm{H}}\} = \mathsf{E}\{\boldsymbol{b}\tilde{\boldsymbol{b}}^{\mathrm{H}}\} = \mathsf{E}\{\tilde{\boldsymbol{b}}\tilde{\boldsymbol{b}}^{\mathrm{H}}\} = \boldsymbol{I}_{KN_T} - \boldsymbol{V}$ and $\hat{\boldsymbol{R}} = \hat{\boldsymbol{S}}^{\mathrm{H}}\hat{\boldsymbol{S}}$.

$$\begin{aligned} (c) \quad & \mathsf{E}\{\boldsymbol{b}\boldsymbol{b}^{\mathrm{H}}\} = \boldsymbol{I}_{KN_T} \\ (b) \quad & \boldsymbol{b}\hat{\boldsymbol{x}}^{\mathrm{H}}\hat{\boldsymbol{F}} = \boldsymbol{b}\left(\hat{\boldsymbol{y}}^{\mathrm{H}}\hat{\boldsymbol{S}} - \tilde{\boldsymbol{b}}^{\mathrm{H}}(\hat{\boldsymbol{R}} - \hat{\boldsymbol{D}})\right)\hat{\boldsymbol{F}} \\ & \qquad = \boldsymbol{b}\left(\boldsymbol{b}^{\mathrm{H}}\hat{\boldsymbol{R}} + \boldsymbol{z}^{\mathrm{H}}\hat{\boldsymbol{S}} - \tilde{\boldsymbol{b}}^{\mathrm{H}}(\hat{\boldsymbol{R}} - \hat{\boldsymbol{D}})\right)\hat{\boldsymbol{F}} \\ & \mathsf{E}\{\boldsymbol{b}\hat{\boldsymbol{x}}^{\mathrm{H}}\hat{\boldsymbol{F}}\} = (\boldsymbol{V}\hat{\boldsymbol{R}} - \boldsymbol{V}\hat{\boldsymbol{D}} + \hat{\boldsymbol{D}})\hat{\boldsymbol{F}} = \boldsymbol{M}_1\hat{\boldsymbol{F}} \\ (a) \quad & \hat{\boldsymbol{F}}^{\mathrm{H}}\hat{\boldsymbol{x}}\hat{\boldsymbol{x}}^{\mathrm{H}}\hat{\boldsymbol{F}} = \hat{\boldsymbol{F}}^{\mathrm{H}}\Big(\hat{\boldsymbol{S}}^{\mathrm{H}}\hat{\boldsymbol{y}}\hat{\boldsymbol{y}}^{\mathrm{H}}\hat{\boldsymbol{S}} + (\hat{\boldsymbol{R}} - \hat{\boldsymbol{D}})\tilde{\boldsymbol{b}}\tilde{\boldsymbol{b}}^{\mathrm{H}}(\hat{\boldsymbol{R}} - \hat{\boldsymbol{D}}) \\ & \qquad - (\hat{\boldsymbol{R}} - \hat{\boldsymbol{D}})\tilde{\boldsymbol{b}}\hat{\boldsymbol{y}}^{\mathrm{H}}\hat{\boldsymbol{S}} - \hat{\boldsymbol{S}}^{\mathrm{H}}\hat{\boldsymbol{y}}\tilde{\boldsymbol{b}}^{\mathrm{H}}(\hat{\boldsymbol{R}} - \hat{\boldsymbol{D}})\Big)\hat{\boldsymbol{F}}. \end{aligned} \tag{60}$$

Taking now the expectation of (a), and knowing that

$$\begin{aligned} \mathsf{E}\{\hat{\boldsymbol{y}}\hat{\boldsymbol{y}}^{\mathrm{H}}\} &= \mathsf{E}\left\{(\hat{\boldsymbol{S}}\boldsymbol{b} + \boldsymbol{z})(\boldsymbol{b}^{\mathrm{H}}\hat{\boldsymbol{S}}^{\mathrm{H}} + \boldsymbol{z}^{\mathrm{H}})\right\} \\ &= \hat{\boldsymbol{S}}\hat{\boldsymbol{S}}^{\mathrm{H}} + \sigma_z^2\boldsymbol{I}_N \\ \mathsf{E}\{\hat{\boldsymbol{y}}\tilde{\boldsymbol{b}}^{\mathrm{H}}\} &= \mathsf{E}\left\{(\hat{\boldsymbol{S}}\boldsymbol{b} + \boldsymbol{z})\tilde{\boldsymbol{b}}^{\mathrm{H}}\right\} = \hat{\boldsymbol{S}}\left(\boldsymbol{I}_{KN_T} - \boldsymbol{V}\right) \end{aligned} \tag{61}$$

we obtain

$$\begin{aligned} \mathsf{E}\{\hat{\boldsymbol{F}}^{\mathrm{H}}\hat{\boldsymbol{x}}\hat{\boldsymbol{x}}^{\mathrm{H}}\hat{\boldsymbol{F}}\} &= \hat{\boldsymbol{F}}^{\mathrm{H}}\left(\hat{\boldsymbol{R}}\boldsymbol{V}\hat{\boldsymbol{R}} + \sigma_z^2\hat{\boldsymbol{R}} + \hat{\boldsymbol{D}}\left(\boldsymbol{I}_{KN_T} - \boldsymbol{V}\right)\hat{\boldsymbol{D}}\right)\hat{\boldsymbol{F}} \\ &= \hat{\boldsymbol{F}}^{\mathrm{H}}\boldsymbol{M}_2\hat{\boldsymbol{F}}. \end{aligned} \tag{62}$$

Combining (a), (b), and (c), the expectation of (59) becomes

$$\begin{aligned} &\mathsf{E}\left\{\|\hat{\boldsymbol{F}}^{\mathrm{H}}\hat{\boldsymbol{x}} - \boldsymbol{b}\|^2\right\} \\ &\qquad = \mathrm{tr}\left\{\boldsymbol{I}_{KN_T} - \hat{\boldsymbol{F}}^{\mathrm{H}}\boldsymbol{M}_1^{\mathrm{H}} - \boldsymbol{M}_1\hat{\boldsymbol{F}} + \hat{\boldsymbol{F}}^{\mathrm{H}}\boldsymbol{M}_2\hat{\boldsymbol{F}}\right\}. \end{aligned} \tag{63}$$

The matrix $\boldsymbol{M}_2$ is hermitian and invertible, thus we can write

$$\begin{aligned} \mathsf{E}\left\{\|\hat{\boldsymbol{F}}^{\mathrm{H}}\hat{\boldsymbol{x}} - \boldsymbol{b}\|^2\right\} &= \mathrm{tr}\left\{\boldsymbol{I}_{KN_T} - \boldsymbol{M}_1\boldsymbol{M}_2^{-1}\boldsymbol{M}_1^{\mathrm{H}}\right. \\ &\quad \left. + \left(\hat{\boldsymbol{F}} - \boldsymbol{M}_2^{-1}\boldsymbol{M}_1^{\mathrm{H}}\right)^{\mathrm{H}}\boldsymbol{M}_2\left(\hat{\boldsymbol{F}} - \boldsymbol{M}_2^{-1}\boldsymbol{M}_1^{\mathrm{H}}\right)\right\}. \end{aligned} \tag{64}$$

This expression is minimized when $\hat{\boldsymbol{F}} - \boldsymbol{M}_2^{-1}\boldsymbol{M}_1^{\mathrm{H}} = \boldsymbol{0}$, leading to $\hat{\boldsymbol{F}} = \boldsymbol{M}_2^{-1}\boldsymbol{M}_1^{\mathrm{H}}$ and

$$\hat{\boldsymbol{F}}^{\mathrm{H}} = (\boldsymbol{V}\hat{\boldsymbol{R}} - \boldsymbol{V}\hat{\boldsymbol{D}} + \hat{\boldsymbol{D}})\left(\hat{\boldsymbol{R}}\boldsymbol{V}\hat{\boldsymbol{R}} + \sigma_z^2\hat{\boldsymbol{R}} + \hat{\boldsymbol{D}}\left(\boldsymbol{I}_{KN_T} - \boldsymbol{V}\right)\hat{\boldsymbol{D}}\right)^{-1}. \tag{65}$$

ACKNOWLEDGMENT

The authors would like to thank R. Müller for his helpful suggestions, as well as the anonymous reviewers for their careful reading of the paper.

REFERENCES

[1] C. F. Mecklenbräuker, J. Wehinger, T. Zemen, H. Artés, and F. Hlawatsch, "Multiuser MIMO channel equalization," in *Smart Antennas—State-of-the-Art*, ser. EURASIP Book Series on Signal Processing and Communications, T. Kaiser, A. Bourdoux, H. Boche, J. R. Fonollosa, J. B. Andersen, and W. Utschick, Eds. New York: Hindawi, 2006, ch. 1.4, pp. 53–76.

[2] T. Zemen, C. F. Mecklenbräuker, J. Wehinger, and R. R. Müller, "Iterative joint time-variant channel estimation and multi-user detection for MC-CDMA," *IEEE Trans. Wireless Commun.*, vol. 5, no. 6, pp. 1469–1478, Jun. 2006.

[3] T. Zemen, "OFDM multi-user communication over time-variant channels," Ph.D. dissertation, Vienna Univ. of Technology, Vienna, Austria, Jul. 2004.

[4] H. van der Vorst, *Iterative Krylov Methods for Large Linear Systems*. Cambridge, U.K.: Cambridge Univ. Press, 2003.

[5] Y. Saad, *Iterative Methods for Sparse Linear Systems*, 2nd ed. Philadelphia, PA: SIAM, 2003.

[6] T. K. Moon and W. Stirling, *Mathematical Methods and Algorithms*. Englewood Cliffs, NJ: Prentice-Hall, 2000.

[7] T. Kailath and A. H. Sayed, *Fast Reliable Algorithms for Matrices With Structure*. Philadelphia, PA: SIAM, 1999.

[8] B. Kecicioglu and M. Torlak, "Reduced rank beamforming methods for SDMA/OFDM communications," in *Proc. 38th Asilomar Conf. Signals, Systems, Computers*, Jul. 12, 2004, vol. 2, pp. 1973–1977.

[9] I. P. Kirsteins and G. Hongya, "Performance analysis of Krylov space adaptive beamformers," in *Proc. IEEE Workshop Sensor Array Multichannel Signal*, Jul. 12, 2006, vol. 3, pp. 16–20.

[10] L. Cottatellucci, R. Müller, and M. Debbah, "Linear detectors for multiuser systems with correlated spatial diversity," presented at the 14th Eur. Signal Processing Conf. (EUSIPCO), Florence, Italy, Sep. 2006.

[11] G. Dietl and W. Utschick, "Complexity reduction of iterative receivers using low-rank equalization," *IEEE Trans. Signal Process.*, vol. 55, no. 3, pp. 1035–1046, Mar. 2007.

[12] L. R. Bahl, J. Cocke, F. Jelinek, and J. Raviv, "Optimal decoding of linear codes for minimizing symbol error rate," *IEEE Trans. Inf. Theory*, vol. 20, no. 2, pp. 284–287, Mar. 1974.

[13] M. Honig, G. Woodward, and Y. Sun, "Adaptive iterative multiuser decision feedback detection," *IEEE Trans. Wireless Commun.*, vol. 3, no. 2, pp. 477–485, Mar. 2004.

[14] S. Hanly and D. Tse, "Resource pooling and effective bandwidths in CDMA networks with multiuser receivers and spatial diversity," *IEEE Trans. Inf. Theory*, vol. 47, no. 4, pp. 1328–1351, May 2001.

[15] C. Dumard, F. Kaltenberger, and K. Freudenthaler, "Low-cost LMMSE equalizer based on Krylov subspace methods for HSDPA," *IEEE Trans. Wireless Commun.*, vol. 6, no. 5, pp. 1610–1614, May 2007.

[16] G. H. Golub and C. F. V. Loan, *Matrix Computations*, 3rd ed. Baltimore, MD: The Johns Hopkins Univ. Press, 1996.

[17] J. Wehinger, "Iterative multi-user receivers for CDMA Systems," Ph.D. dissertation, Vienna Univ. of Technology, Vienna, Austria, Jul. 2005.

[18] P. W. Wolniansky, G. J. Foschini, G. D. Golden, and R. A. Valenzuela, "V—BLAST: An architecture for achieving very high data rates over rich-scattering wireless channels," presented at the Int. Symp. Signals, Systems, and Electronics (ISSSE), Pisa, Italy, 1998.

[19] C. Dumard and T. Zemen, "Krylov subspace method based low-complexity MIMO multi-user receiver for time-variant channels," presented at the 17th IEEE Int. Symp. Personal, Indoor, Mobile Radio Communication (PIMRC), Helsinki, Finland, Sep. 2006.

[20] S. Verdú, *Multiuser Detection*. New York: Cambridge Univ. Press, 1998.

[21] T. Zemen and C. F. Mecklenbräuker, "Time-variant channel estimation using discrete prolate spheroidal sequences," *IEEE Trans. Signal Process.*, vol. 53, no. 9, pp. 3597–3607, Sep. 2005.

[22] D. Slepian, "Prolate spheroidal wave functions, Fourier analysis, and uncertainty—V: The discrete case," *Bell Syst. Tech. J.*, vol. 57, no. 5, pp. 1371–1430, May–June 1978.

[23] T. Zemen, H. Hofstetter, and G. Steinböck, "Successive Slepian subspace projection in time and frequency for time-variant channel estimation," presented at the 14th IST Mobile Wireless Communication Summit (IST SUMMIT), Dresden, Germany, Jun. 19–22, 2005.

[24] L. M. Correia, *Wireless Flexible Personalised Communications*. New York: Wiley, 2001.

[25] R. H. Clarke, "A statistical theory of mobile-radio reception," *Bell Syst. Tech. J.*, vol. 47, pp. 957–1000, Jul./Aug. 1968.

[26] L. Hanzo, T. H. Liew, and B. L. Yeap, *Turbo Coding, Turbo Equalization and Space-Time Coding for Transmission Over Fading Channels*. New York: Wiley, 2002.

Charlotte Dumard (S'05) was born in Paris, France. She received a double Master's of Science degree from the Royal Institute of Technology (KTH), Stockholm, Sweden, and the École Supérieure d'Électricité (Supélec), Gif-sur-Yvette, France, both in 2002. Since February 2006, she has been working towards the Ph.D. degree at the Vienna University of Technology, Vienna, Austria.

Since September 2004, she has been with the Telecommunications Research Center Vienna (ftw.), working as a Junior Researcher on the project Future Mobile Communications Systems—Mathematical Modeling, Analysis, and Algorithms for Multi Antenna Systems, which is funded by the Vienna Science and Technology Fund (Wiener Wissenschafts-, Forschungs- und Technologiefonds, WWTF). Her research interest are low-complexity transceiver design in time-varying MIMO channels as well as distributed signal processing.

Thomas Zemen (S'03–M'05) was born in Mödling, Austria. He received the Dipl.-Ing. degree (with distinction) in electrical engineering and the doctoral degree (with distinction), both from the Vienna University of Technology, Vienna, Austria, in 1998 and 2004, respectively.

He joined Siemens Austria in 1998, where he worked as a Hardware Engineer and Project Manager for the Radio Communication Devices Department. He engaged in the development of a vehicular GSM telephone system for a German car manufacturer. From October 2001 to September 2003, he was delegated by Siemens Austria as a Researcher to the Mobile Communications Group at the Telecommunications Research Center Vienna (ftw.). Since October 2003, he has been with the Telecommunications Research Center Vienna, working as researcher in the strategic I0 project. His research interests include orthogonal frequency division multiplexing (OFDM), multiuser detection, time-variant channel estimation, iterative MIMO receiver structures, and distributed signal processing. Since May 2005, he has led the project Future Mobile Communications Systems—Mathematical Modeling, Analysis, and Algorithms for Multi Antenna Systems, which is funded by the Vienna Science and Technology Fund (Wiener Wissenschafts-, Forschungs- und Technologiefonds, WWTF). He teaches MIMO Communications as an external Lecturer at the Vienna University of Technology.